[redacted] Security Information

AN EVALUATION OF A METHOD OF IMPROVING THE TAKE-OFF CHARACTERISTICS OF CATAPULT-LAUNCHED JET AIRPLANES

A Thesis

Presented to

the Faculty of the Department of Engineering

University of Virginia

In Partial Fulfillment

of the Requirements for the Degree

Master of Aeronautical Engineering

---

by

[redacted] Wilmer H. Reed

June 1953

AN EVALUATION OF A METHOD OF IMPROVING THE TAKE-OFF CHARACTERISTICS OF CATAPULT-LAUNCHED JET AIRPLANES

A Thesis

Presented to

the Faculty of the Department of Engineering

University of Virginia

In Partial Fulfillment

of the Requirements for the Degree

Master of Aeronautical Engineering

---

by

Wilmer H. Reed

June 1953

APPROVAL SHEET

This thesis is submitted in partial fulfillment of the requirements for the degree of Master of Aeronautical Engineering

_____
Author

Approved:

_____
Faculty Advisor

_____
For Subcommittee

_____
Chairman, Committee on Graduate Studies in Engineering

June 1953

TABLE OF CONTENTS

LIST OF TABLES

LIST OF FIGURES

CHAPTER I

STATEMENT OF THE PROBLEM

The tendency of some of the modern carrier based airplanes to lose height after being catapult launched from carrier decks has become a problem of growing concern to the Navy. Several types of jet fighter airplanes in current use by the fleet have exhibited marginal take-off performance when catapulted, and others, now in the design and development stage, are expected to have even more critical catapult take-off characteristics.

This loss in height subsequent to take-off may be attributed largely to the combined effects associated with the use of low-aspect-ratio wings, small ground attitude angles, and high wing loadings. The low lift-curve slopes representative of low-aspect-ratio delta-wing configurations require that the angle of attack be quite high at presently available launching speeds. The angle of attack at maximum lift for such wing plan forms may be 20° or greater. Because present-day launching speeds are higher than the airplane stall speed, the problem resolves itself into being able to obtain the required high trim angle of attack before settling occurs. In addition, the tricycle landing gears used on jet aircraft generally provide static ground attitude angles which are considerably less than the angle

of attack associated with maximum lift. When these features are combined in an airplane configuration, as they frequently are with modern jet airplanes, the lift developed at the instant the wheels leave the end of the deck may be appreciably less than the weight of the airplane, even when its launching speed is 10 per cent or more above minimum flight speed. In such cases it is necessary that the pilot, by use of longitudinal controls, pitch the airplane to the required angle of attack in time sufficient to prevent an excessive loss in height.

Although a carrier flight deck is usually from 50 to 70 feet above the water line, any apparent uncontrollable tendency of the airplane to lose height after being launched is a source of considerable anxiety to the pilot, especially during night catapult operations where the surface of the sea is generally not visible.

Modified launching procedures. Various modifications of existing catapult launching techniques and procedures together with special catapulting devices have been considered in order to improve the launching characteristics of airplanes expected to have critical take-off performance. Among these special catapulting arrangements are

(a) Dynamically rotating the airplane during the catapult power stroke by utilizing the

catapult force to impart a nose-up pitching moment. This procedure might be difficult to control with varying airplane loadings and inconsistencies in the time histories of the catapult force.

(b) Fixing the airplane at a higher-than-normal ground attitude angle by either extending the nose-wheel oleo strut or holding the tail down prior to the catapult power stroke.

This arrangement introduces problems associated with the inclination of the jet exhaust, such as increased difficulty and hazard to the spotting crew and considerable heating of the flight deck in the vicinity of the catapult holdback position. It may also increase the time required for spotting the airplane on the catapult.

Method considered by thesis. In view of the disadvantages associated with the preceding modified catapulting arrangements, an alternate method is considered in the present paper. The method incorporates the installation of a curved ramp on the portion of the deck extending from the bridle release point to the bow end of the deck, a distance of 50 feet. The primary function of such a ramp would be to impart an initial vertical velocity to the catapulted airplane in order that more time would be available for the

controls to pitch the airplane to the required angle of attack before settling could occur. The speed reduction sacrificed to obtain the required initial vertical velocity appears to be of little consequence with present-day catapulting equipment. In cases where the elevator control effectiveness is low, the curvature of the ramp would also provide an additional nose up pitching velocity and thereby reduce the time required to reach the trim angle of attack.

To illustrate the effect of such a ramp, the take-off characteristics of a conventional straight-wing jet fighter airplane of moderate aspect ratio and a low-aspect-ratio delta-wing airplane are calculated, assuming in one case, the airplane traverses a flat deck and in the other, a curved ramp. The curved ramp considered is of circular-arc profile and has a total rise of 1.73 feet in its length of 50 feet.

CHAPTER II

THE PROCEDURE USED AND THE EXAMPLES CONSIDERED

The present investigation is concerned with motion of an airplane over an interval extending from the point at which the catapult bridle is released to a position ahead of the carrier where the transient effects of the take-off have largely subsided. It is in this interval, a period of approximately 2 seconds, that the pilot may have little or no control over the airplane's motion.

Essentially, the computational procedure involved solving three simultaneous equations of airplane motion with prescribed initial conditions determined at the instant the wheels leave the deck. In order to simplify the analysis, the landing gear was assumed to be rigid and in all but one case the controls were considered to be locked. The derivation of equations and a detailed discussion of their application may be found in the appendix.

The curved ramp. The ramp used as an example in the following computations has a circular-arc profile with a radius of 720 feet; it is tangent to and extends 50 feet beyond the catapult release point. The total rise of the ramp is 1.73 feet and the width is sufficient so that the main wheels as well as the nose wheel will follow its

surface. With a catapult end speed of 85 knots, the pitching velocity of an airplane traversing the ramp is 11° per second, the normal acceleration sustained by the airplane is 1.9g, and the vertical velocity of the wheels at the end of the ramp is 10 feet per second. The sketch shown in Figure 1 gives an indication of the size of the ramp compared with a conventional jet fighter airplane. It might be noted that since the normal acceleration imparted by a circular-arc ramp is constant, a circular arc provides the least possible maximum acceleration required for a given vertical velocity at the end of the ramp.

Airplanes used as examples. Two airplanes have been chosen to illustrate the effect of the curved ramp.

Airplane A is a straight-wing fighter airplane with moderate aspect ratio. The physical characteristics and the aerodynamic data obtained from a wind-tunnel test of airplane A are presented in table I. Longitudinal control is provided by elevators mounted on a conventional horizontal tail.

Airplane B is a low-aspect-ratio, tailless configuration with a modified delta-wing plan form. The physical characteristics and wind-tunnel data used with the computations for airplane B are also given in table I. Longitudinal control is accomplished by elevons and trimmers

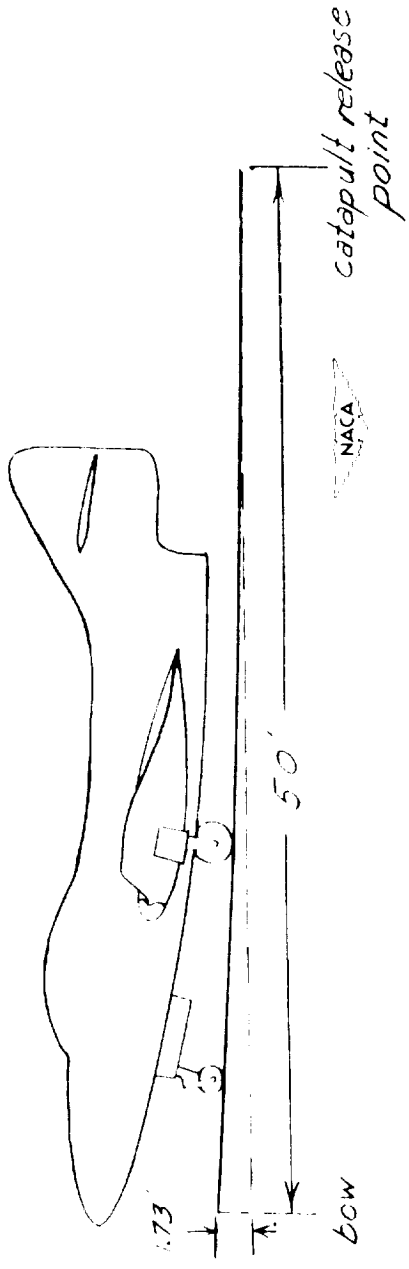

FIGURE 1

GEOMETRY AND RELATIVE SIZE OF THE CIRCULAR-ARC RAMP AND A CONVENTIONAL FIGHTER AIRPLANE

TABLE I

CHARACTERISTICS OF AIRPLANES USED IN CALCULATIONS

Characteristic	Airplane A	Airplane B
W, lb	13,000	19,000
m, slugs	403.9	590.0
k_Y, ft	6.68	7.30
V_c, knots	85	88
U, knots	10	25
T, lb	5,000	8,000
S, sq ft	260	557
A	4.30	2.07
$\bar{c}$, ft	7.45	18.25
Center-of-gravity location, percent mean aerodynamic chord	25.5	22.0
l_m, ft	1.5	1.9
h_m, ft	3.1	5.2
l_t, ft	------	12.0
h_t, ft	------	2.8
l_n, ft	12.0	14.3

NACA

TABLE I.- Concluded

CHARACTERISTICS OF AIRPLANES USED IN CALCULATIONS

Characteristic	Airplane A	Airplane B	
	Without ground effect	Without ground effect	With ground effect
C_{L_0}	0.53	-0.11	-0.22
C_{L_α}, per radian	4.27	2.64	3.67
$C_{L_{\delta_e}}$, per radian	0.57	0.49	0.52
C_{D_0}	0.11	0.00[a]	0.040
e	0.735	0.422	0.830
C_{m_0}	0.028	0.058	0.103
$\frac{dC_m}{dC_L}$	-0.050	-0.120	-0.164
C_{m_α}, per radian	-0.214	-0.316	-0.565
$C_{m_{\delta_e}}$, per radian	-1.080	-0.271	-0.291
C_{m_q}	-12.70	-0.70	-0.70
$C_{m_{D\alpha}}$	-5.08	0	0

[a]The experimental variation of C_D with C_L^2 was nonlinear and had a value of C_{D_0} of 0.04. The closest linear approximation to the experimental data, particularly at the higher lift coefficients, involved using a value of C_{D_0} of zero.

NACA

located at the trailing edge of the wing. A tail wheel has been added to the tricycle-type landing gear to prevent structural damage to the tail when taking off and landing at high attitude angles. The static attitude angle of this configuration is only 2.7°; however, it is possible to attain 7.0° by pumping the nose-wheel oleo strut to its fully extended position, or 14.0° by fixing the airplane in a tail-down position with the tail-wheel oleo strut fully compressed.

Assumed catapult and wind speeds. Take-off calculations have been carried out assuming an 85-knot catapult end speed for both airplanes and a wind speed over the deck of 10 knots for the case of airplane A and 25 knots for airplane B. With these launching speeds, the lift deficiency on leaving the straight deck was 25 per cent for airplane A (attitude angle, 7.4°) and 38 per cent for airplane B (attitude angle, 14.0°). A 25-knot wind speed is the minimum normally considered for carrier operations; however, the 10-knot speed was used for airplane A to illustrate the effect of the ramp with this configuration under a critical condition.

CHAPTER III

RESULTS AND DISCUSSION

Launching characteristics of airplane A. The computed variations in height, normal acceleration, angle of attack, vertical velocity, true airspeed, and attitude angle with horizontal distance relative to the carrier and referred to the catapult release point are shown in Figure 2 for the case of airplane A launched from a straight deck and the curved ramp. An approximate time scale determined from the mean of the velocities in the two cases is also included in Figure 2.

In addition to the airplane characteristics listed in table I, airplane A was assumed to have a fixed elevator deflection of -2.0°. With the center-of-gravity location considered (5 per cent static margin), this elevator deflection will provide steady trimmed flight at $0.9C_{L_{max}}$. The attitude angle relative to the take-off platform is 7.40° and is the static angle. Since the landing gear is assumed to be rigid and the aerodynamic pitching moment, in this case, is less than the moment required to lift the nose wheel, the attitude angle relative to the deck remains constant until the nose wheel leaves the end of the deck. The airplane then acquires a nose-down pitching acceleration which is sustained until the main wheels leave the end of

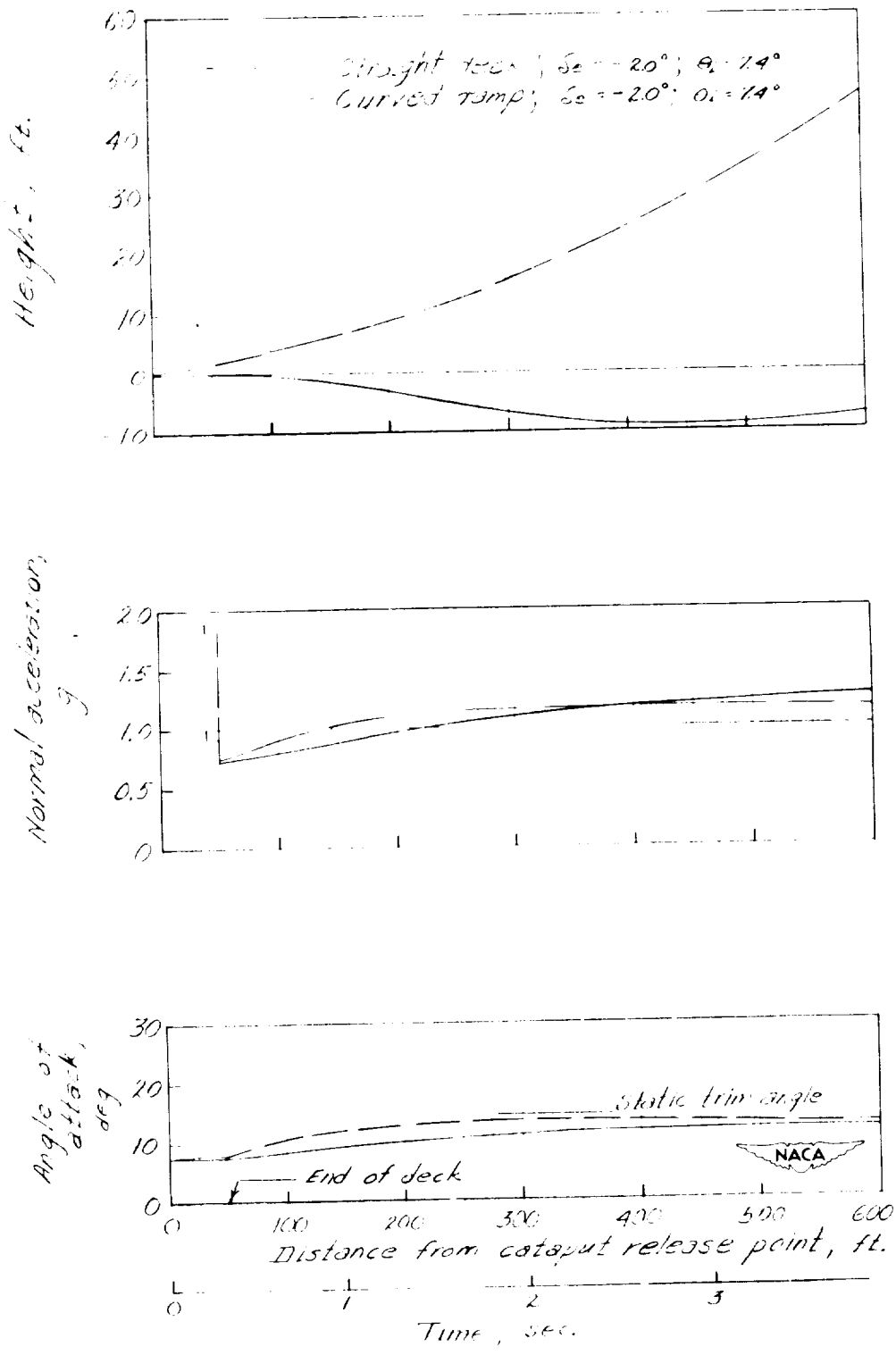

FIGURE 2

CALCULATED TAKE-OFF CHARACTERISTICS OF AIRPLANE A. $\delta_e = -2.0^\circ$ AND $\theta_i = 7.4^\circ$ FOR THE STRAIGHT DECK AND CURVED RAMP

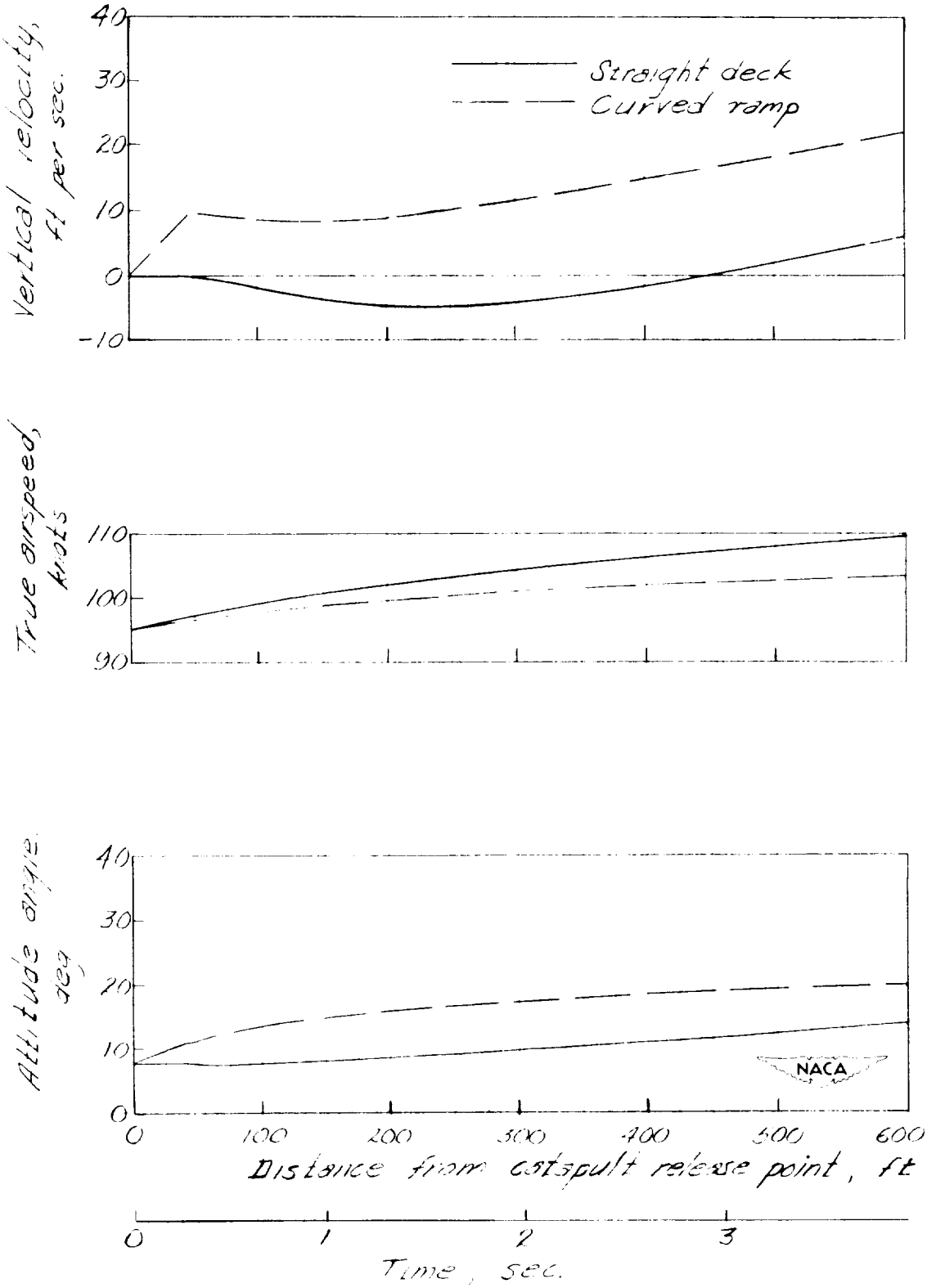

FIGURE 2

CONCLUDED

the deck. The reduced downwash at the tail caused by aerodynamic ground effect would increase this nose-down pitching acceleration, but ground effect was neglected for the case of airplane A, since its influence on pitching is of such brief duration.

It is seen from the normal acceleration time histories in Figure 2 that, in both cases, the lift developed immediately after the main wheels leave the deck is approximately 75 per cent of the required lift. While the airplane in the straight deck case begins to lose altitude as a result of this lift deficiency, it continues to climb when launched from the ramp by virtue of the initial upward momentum imparted by the ramp. The greater rate of climb in this case is, of course, accompanied by a reduced rate of increase in forward speed, since the thrust produced is the same in both cases. It appears, however, that the forward speed sacrificed in order to gain height is of little consequence because, as indicated by the time histories of true airspeed, the airspeed continues to increase from its initial value, a speed which provided a safe margin above the stalling speed.

In addition to the favorable effect of the initial upward translational velocity, the ramp also imparted a nose-up pitching velocity which reduced the time required to accelerate upward by a factor of approximately one-half.

Although the pitching velocity imparted by the ramp is 11.0° per second when three wheels are in contact with the ramp, it is reduced somewhat during the interval while the nose wheel is ahead of the end of the ramp and the main wheels are in contact with its surface. In the present example, the pitching velocity was reduced to 7.6° per second.

The plot of airplane height variations with distance from the carrier reveals the important result that, due to an initial insufficient lift, a loss of height of 9 feet is experienced by the airplane when launched from a conventional straight deck, whereas under similar conditions the airplane launched from a curved ramp shows no tendency to settle, but continues to climb. Three seconds after take-off, the vertical spread between the flight paths of the two cases is approximately 40 feet.

The angle of attack of airplane A did not reach the static trim value $\left(0.9C_{L_{max}}\right)$ for which the controls were set throughout the time interval covered by the computations; however, for some conditions where there may be danger of exceeding the stall angle of attack, it may be necessary to use a reduced control deflection with curved ramp launchings. Inasmuch as the angle of attack reached by the straight deck case is less than that for the ramp, it may be possible that some gain could be realized without danger of overshooting the stall angle by setting the

controls for the straight-deck case at a somewhat higher trim angle of attack and thereby increase the aerodynamic pitching moment. It is felt, however, that this change would not greatly alter the comparison.

Launching characteristics of airplane B. A presentation of the take-off characteristics of airplane B launched from a straight deck and the curved ramp is given in Figures 3 and 4. The computed variables are the same as those for airplane A in Figure 2.

In some cases, the aerodynamic pitching moment of airplane B was sufficient to lift the nose wheel immediately after release of the catapult bridle. Aerodynamic ground effect would, in such cases, affect the pitching over the entire length of the 50-foot take-off run, and was therefore taken into account during the take-off run of airplane B. The aerodynamic characteristics of airplane B with ground effect were taken from wind-tunnel tests and are given in table I.

Figure 3 shows the case wherein the control deflection is -9.0° and the attitude angle at the bridle release point is 7.0°, the angle obtained by blocking the nose-wheel oleo strut to its fully extended position.

The aerodynamic pitching moment was sufficient to lift the nose wheel during the straight-deck take-off run,

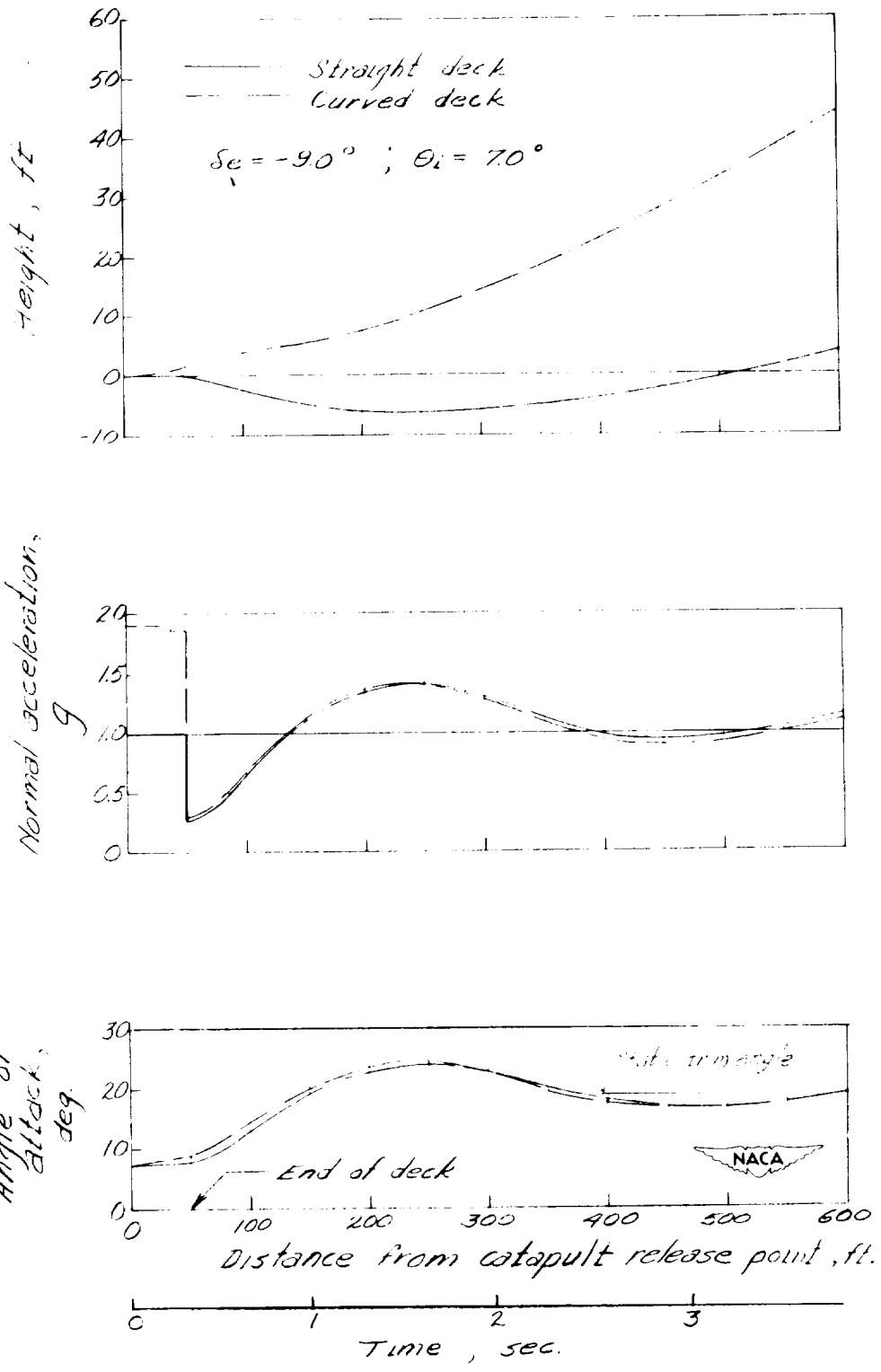

FIGURE 3

CALCULATED TAKE-OFF CHARACTERISTICS OF AIRPLANE B. $\delta_e = -9.0°$ AND $\theta_i = 7.0°$ FOR THE STRAIGHT DECK AND CURVED RAMP

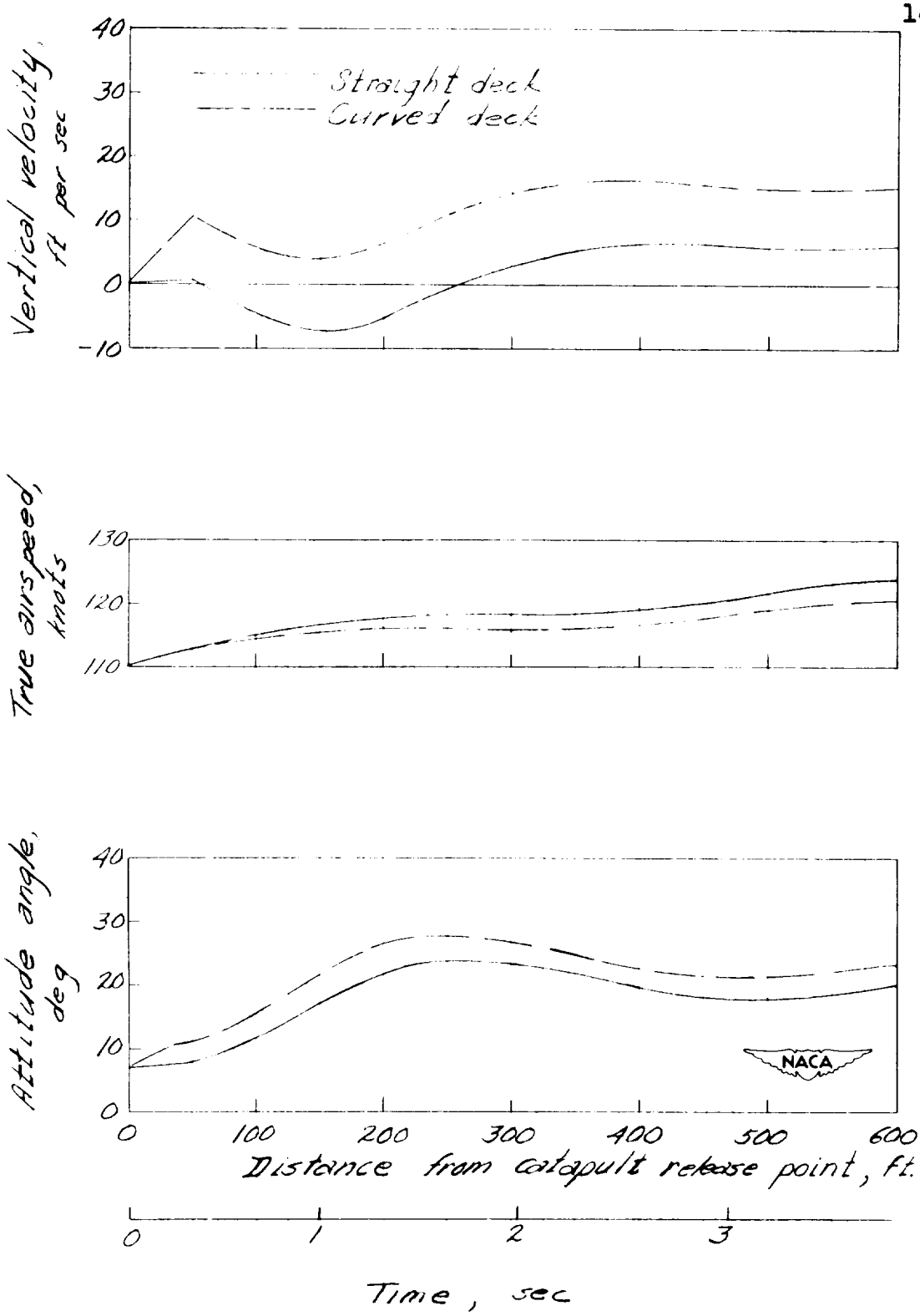

FIGURE 3

CONCLUDED

[redacted]

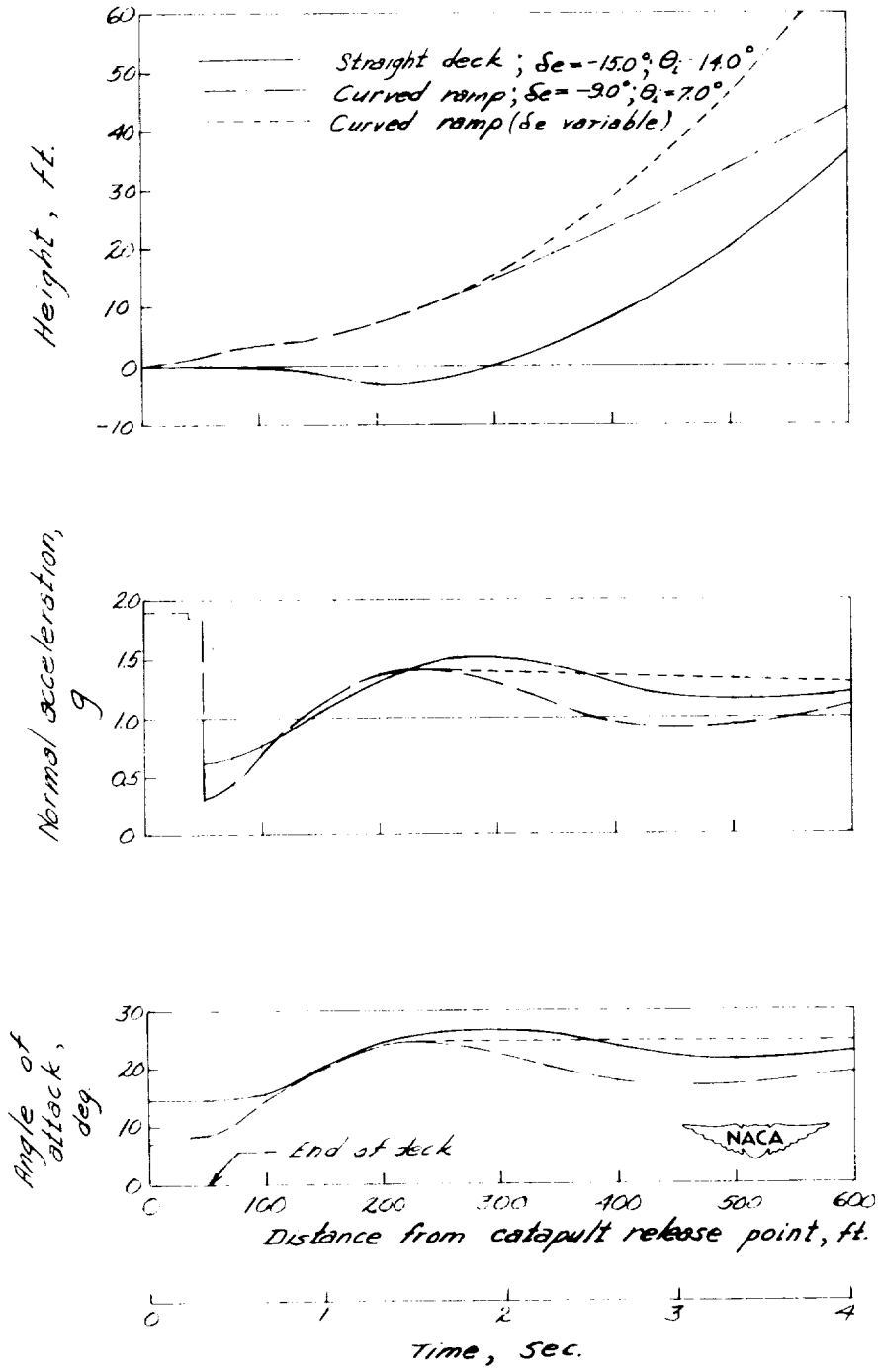

FIGURE 4

CALCULATED TAKE-OFF CHARACTERISTICS OF AIRPLANE B. $\delta_e = -15.0^\circ$ AND $\theta_i = 14.0^\circ$ FOR THE STRAIGHT DECK AND $\delta_e = -9.0^\circ$ AND $\theta_i = 7.0^\circ$ FOR CURVED RAMP. ALSO SHOWN IS THE CASE WHERE THE CONTROL DEFLECTION IS VARIED SO THAT THE ANGLE OF ATTACK REMAINS CONSTANT AT ITS PEAK VALUE

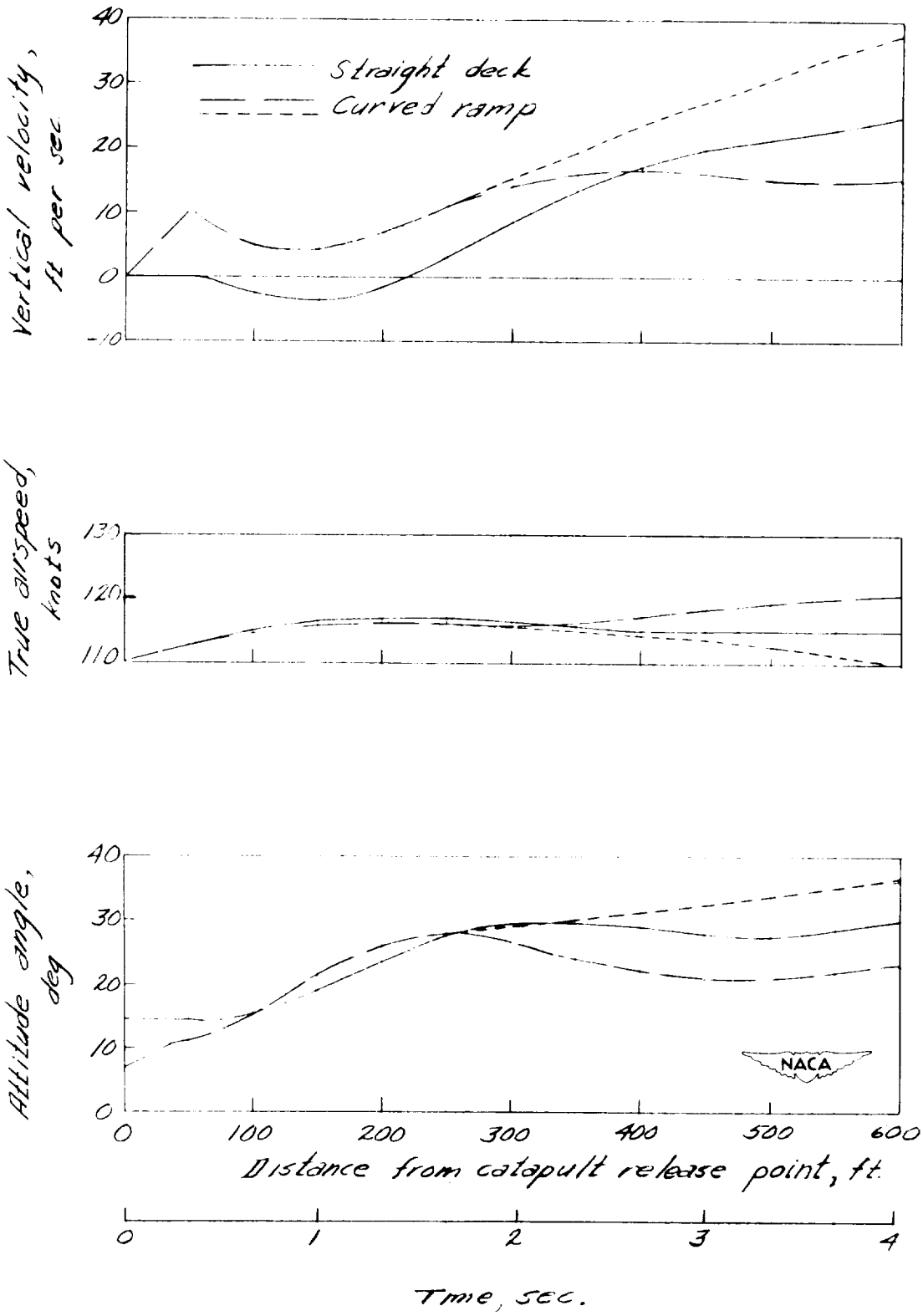

FIGURE 4

[redacted]

but, due to the radial ramp acceleration acting at the center of gravity which is forward of the main wheels, the same aerodynamic pitching moment was not sufficient to lift the nose wheel for the case of the curved ramp. As a result, the nose-up pitching velocity at the instant of take-off is 4.4° per second for the straight deck as compared with 7.0° per second for the curved ramp. Since the difference in nose-up pitching velocity at the instant of take-off is small, the potential advantage of the ramp for this case is primarily due to the initial vertical velocity.

The total loss in height following the straight-deck take-off is 6 feet and the airplane remains below deck level for a distance of about 450 feet. The airplane after taking off from the curved ramp continues to climb and, in a distance of 500 feet from the carrier bow, has attained a height 36 feet greater than the straight-deck case. The minimum rates of climb for the case of the curved ramp and straight deck are, respectively, 4 and -8 feet per second.

In Figure 4 the ramp launching shown in the preceding figure is compared with a launching from the straight deck in which the initial attitude angle is 14.0° and the control deflection is -15.0°. Also included in the figure are results of computations made for the ramp case in which the control deflection is fixed at -9.0° until the maximum

angle of attack is reached, at which time the controls are moved in a manner required to hold the angle of attack constant.

It will be noted that in Figure 4 the initial control deflection for the ramp case is less than the deflection used with the straight-deck launching. A reduced control deflection was used in view of the results of other computations for a similar launching from the ramp, wherein the control deflection was -15.0°. Here, it was revealed that with a -15.0° control deflection the initial pitching velocity imparted by the ramp, coupled with the effects of low damping in pitch and a large initial out of trim pitching moment, caused the angle of attack to reach a peak value of 30°, an angle believed to be greater than the stall angle of attack of this airplane. In connection with large angles of attack, it should be mentioned that the analysis assumes a linear variation in lift and pitching moment with angle of attack; consequently, near the stall angle, where this assumption is not valid, the computations are somewhat in error.

Since the straight-deck case has the higher control setting of the two launchings shown in Figure 4, the rate of climb for this case, assuming the controls remained fixed, will eventually exceed that of the ramp. It is possible, however, for the pilot to improve the rate of climb of the

ramp case by increasing the control deflection after there is assurance that the stall angle of attack will not be exceeded. An example is considered wherein the controls are assumed to be fixed at -9.0° until the maximum angle of attack is reached and thereafter are deflected so as to hold the angle of attack constant. This condition could only be approached in the practical case since computations show that the required control motion has the form of a step deflection, increasing from -9.0° to -16.9° at the time the angle of attack reaches a maximum value of 24.3°. The deflection then approaches a steady-state value of -16.5°. The computed results using the foregoing assumption are identified in Figure 4 by the short dashed curves.

In addition to the results presented herein, flight-path computations were also made for a ramp launching of airplane B at a lighter weight (17,000 lb) and at an initial attitude angle of 2.7°. At this angle only 3 per cent of the required lift was developed at the end of the deck. This very low lift at $\alpha = 2.7°$ is associated with an upward trimmer deflection which reduces the lift at a given angle of attack. The initial vertical velocity and the nose-up pitching velocity imparted by the ramp, however, were sufficient to prevent any subsequent loss in height. The minimum vertical velocity in this case was upward 2 feet per second.

CHAPTER IV

A QUALITATIVE ILLUSTRATION OF A SMALL SCALE MODEL CATAPULTED FROM A CURVED RAMP

The preceding computations have indicated that a curved ramp of relatively small height would provide substantial improvement in the launching characteristics of airplanes catapulted with a lift deficiency at the instant of take-off. In order to give a qualitative verification of these trends, motion pictures were made of catapult launchings of a small delta-wing model.[1] No attempt was made in this simple experiment to precisely duplicate full-scale conditions; however, the thrust-weight ratio, the wing plan form, and the ratio of airplane length to ramp length were, in these tests, approximately equivalent to airplane B in the preceding computations. The ground attitude angle and launching speed of the model were so adjusted that a noticeable dip in the flight path resulted when the model was catapulted from a flat launching platform. Similar launchings were then made with various amounts of curvature in the launching platform.

---

[1] The author is grateful to Mr. Marlin Hazen for constructing the model airplane and assisting in the launching demonstrations.

Description of the test apparatus. A sketch of the model, the catapulting device, and the launching technique is presented in Figure 5. The model, constructed of balsa wood, had a delta-wing plan form with a 12-inch span and an aspect ratio of 2.6. Although the model was not powered, a thrust-weight ratio of 0.42 was approximated by referring motion of the model to a reference line which was tilted downward in the direction of flight an angle $\tan^{-1} T/W$ (23°). In this manner, the weight component of the model contributes a constant thrust in the direction of the assumed reference line; however, in the actual case the thrust is constant in the direction of the fuselage reference line. Therefore, the equivalent thrust of the model is less than the thrust would be if the model were actual powered to provide the assumed thrust-weight ratio, by a factor of the cosine of its attitude angle.

The launching platform used to simulate a carrier deck was a 12- by 30-inch sheet of 1/8-inch plywood supported from beneath by a rigid frame (see Figure 5). The platform was bonded to the frame aft of a point 12 inches from the forward end and was free to bend upward ahead of this point. A circular-arc ramp was approximated by simply blocking up the forward end of the flexible platform.

The catapulting device consisted of an elastic shock cord connected, by a suitable pulley arrangement, to a

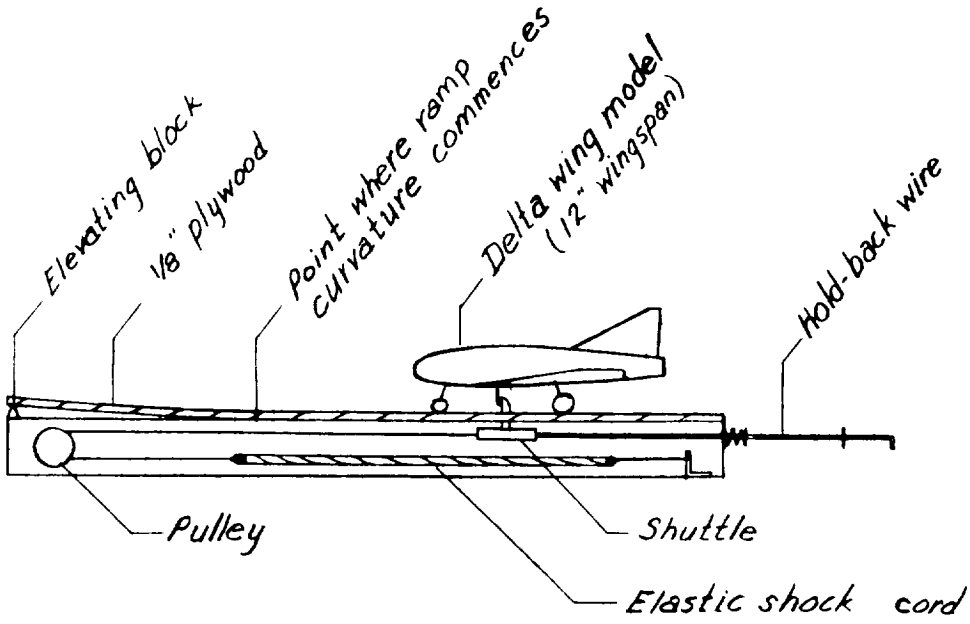

Not to scale

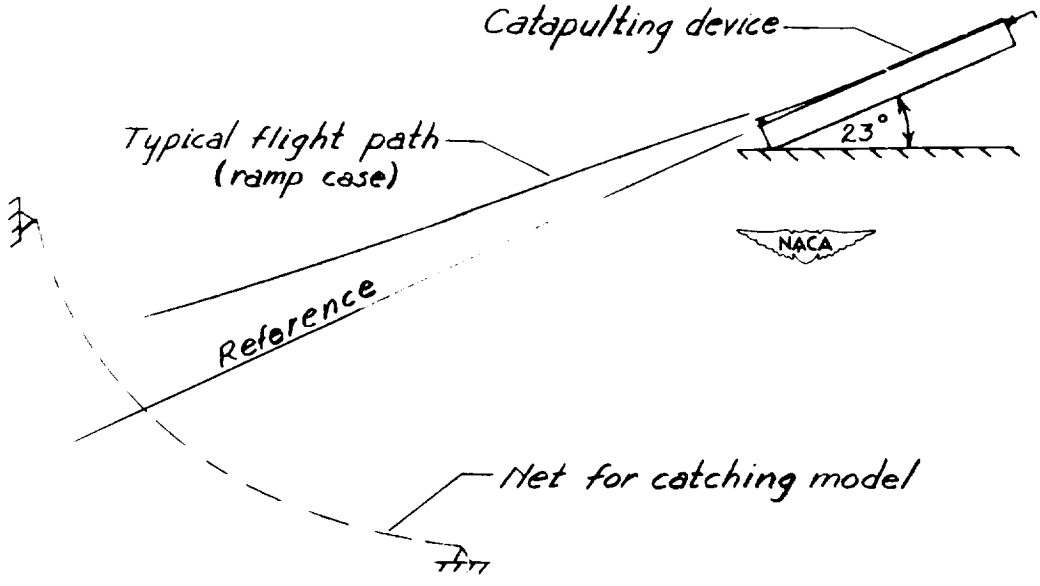

FIGURE 5

SKETCH OF MODEL AND CATAPULTING DEVICE USED TO ILLUSTRATE THE EFFECTS OF A CURVED RAMP

shuttle which was free to slide in a fore and aft direction. Details of its operation are shown in Figure 6.

Results of the test. It was found that the 16-mm motion-picture frames on which the launchings were photographed could not be enlarged for suitable reproduction; therefore, the flight paths and an indication of the attitude angle at various points along the path of typical launchings were obtained from a sequence of such frames and are presented in Figure 6. To avoid confusion, the camera was rotated about its focal axis so that, in the pictures, the tilted reference line appeared to be horizontal. The three cases shown in the figure represent a straight deck launching and curved ramp launchings in which the end of the ramp was elevated 4 and 8 per cent of its length. It might be noted that the circular-arc ramp considered in the computations had a total rise of approximately 3.5 per cent. The launching speeds were essentially the same for each of the three cases.

The trim of the model was the same for both the straight deck case and the 4 per cent ramp case; however, with the 8 per cent ramp launching, the trim angle of attack was reduced somewhat in an attempt to prevent excessive pitching after take-off due to the large initial pitching velocity imparted by the ramp. In view of the high angle of

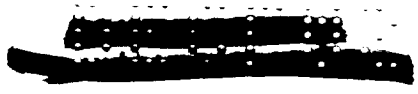

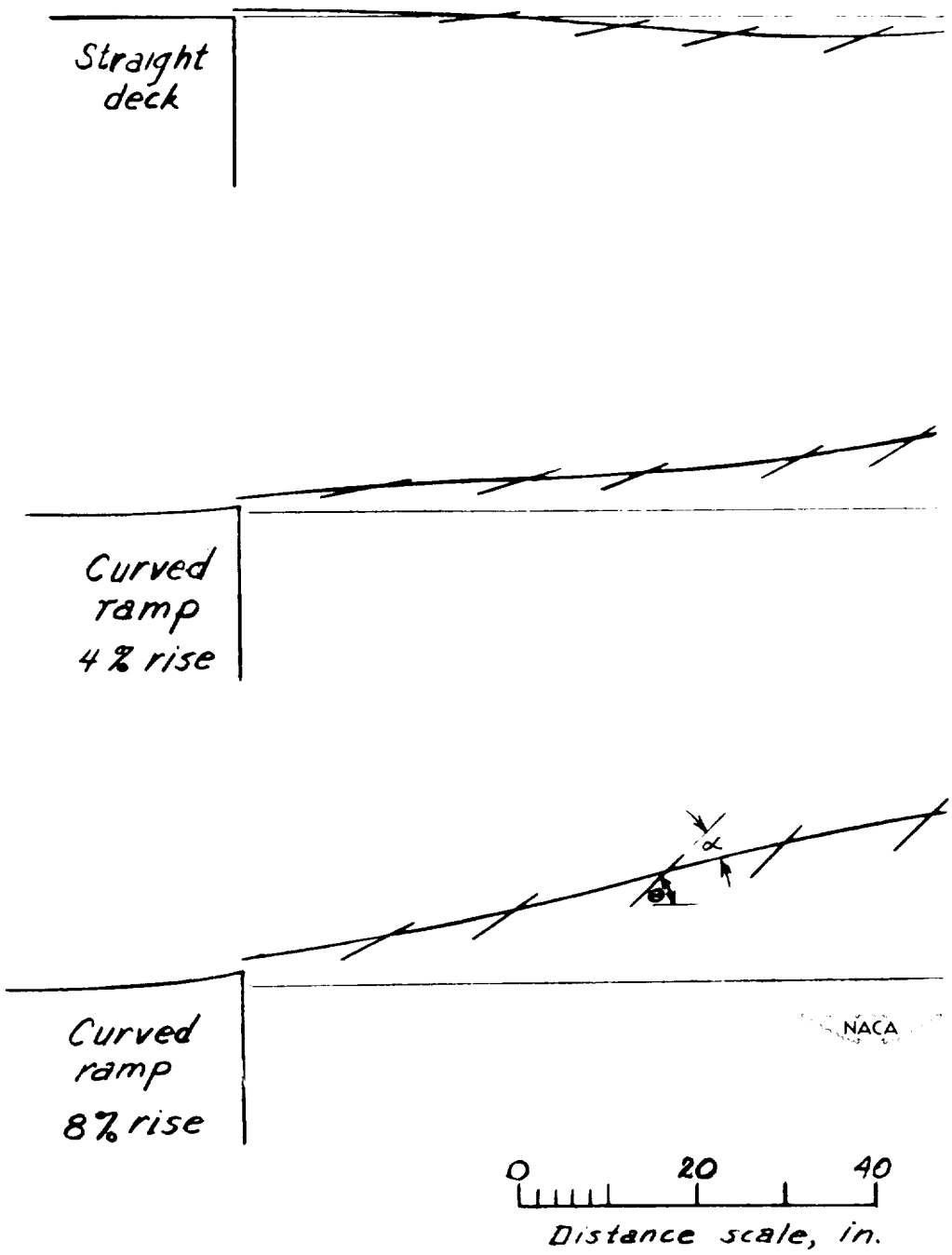

FIGURE 6

A QUALITATIVE INDICATION OF THE FLIGHT PATHS AND ATTITUDE ANGLES OBTAINED FROM MOTION PICTURES OF A CATAPULTED DELTA-WING MODEL HAVING A 12-INCH WING SPAN

attack obtained after take-off in this case, it appears that a further reduction in the trim setting may be desirable, or possibly, it may not be practical to use a ramp of such large curvature in cases where the airplane has low damping in pitch.

In general, the effects of a curved ramp on the model launchings shown in Figure 6 are in qualitative agreement with the trends predicted by calculations in preceding sections of the thesis.

CHAPTER V

CONCLUSIONS

A possible method of improving the take-off performance, in cases where an airplane is catapulted with a lift deficiency at the instant of take-off but at a speed somewhat greater than the stall speed, was considered by the thesis. The method incorporates the installation of a curved ramp over the portion of a carrier deck extending from the catapult release point to the bow end of the flight deck, a distance of 50 feet. The function of the ramp would be to impart an initial upward translational velocity together with a nose-up pitching velocity to the catapulted airplane. The initial vertical velocity would serve to provide more time for increasing the angle of attack before settling could occur, and, in cases where the longitudinal control effectiveness is low, the initial nose-up pitching velocity would reduce the time required to reach the trimmed angle of attack.

The effects of a circular-arc ramp on the take-off characteristics of a straight-wing jet fighter airplane of moderate aspect-ratio and a low-aspect-ratio delta-wing airplane were calculated in the early stages of flight subsequent to being launched at insufficient lift. It was found that a ramp of relatively small height (1.73 feet)

could be used effectively to eliminate the tendency of these airplanes to settle when launched from a conventional straight deck. The amount of height lost in the straight deck launchings considered was as much as 9 feet, whereas with similar launching from the ramp the airplanes remained above deck level and continued to climb. It was noted in certain cases where ramp launchings were computed for the tailless delta-wing airplane that it was necessary to use a reduced control deflection in order to prevent the angle of attack from becoming excessive. This was attributed to the initial nose-up pitching velocity imparted by the ramp in conjunction with the very low damping in pitch which is inherent with tailless configurations.

In addition to these calculations, a simple experiment was conducted in which a delta-wing model having a 12-inch span was launched from a straight and a curved take-off platform. Motion pictures taken of these launchings qualitatively confirmed the trends indicated by the calculations.

SYMBOLS

A	aspect ratio
a_r	radial acceleration of ramp in g units
$\bar{c}$	wing mean aerodynamic chord
C_D	drag coefficient, D/qS
C_L	lift coefficient, L/qS
C_m	pitching-moment coefficient, $M/qS\bar{c}$
D	drag
e	airplane efficiency factor
F	deck reaction force
g	acceleration due to gravity
h	distance between fuselage reference line and wheel hub measured in plane of symmetry, perpendicular to fuselage reference line
k_Y	radius of gyration about lateral axis
L	lift
l	distance between center of gravity and wheel hub measured in plane of symmetry parallel to fuselage reference line
l'	defined by equation (5) of appendix
M	pitching moment (positive nose up)
m	airplane mass
q	dynamic pressure, $\rho V^2/2$
R	radius of curvature of curved ramp

S	wing area
s	distance measured along flight path
t	time
T	thrust
U	wind speed relative to carrier deck
V	true airspeed
V_c	catapult end speed relative to deck
W	airplane weight
x	horizontal distance between catapult-bridle release point and main wheel hub
X	axis in direction of free stream
Z	vertical axis perpendicular to free stream
α	angle of attack
δ_e	elevator or elevon angle
θ	attitude angle
μ	coefficient of friction
ρ	air density
γ	flight-path angle
ϕ	deck angle

Subscripts:

n	nose wheel
m	main wheel
t	tail wheel
1	catapult-bridle release point

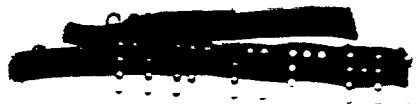

The terms involving a subscript 0 (C_{L_0}, C_{D_0}, and so forth) are the values of the coefficients when the variables upon which they depend are zero. A dot over a variable indicates differentiation with respect to time. Definitions of stability derivatives are given by the following examples:

$$C_{L_\alpha} = \frac{\partial C_L}{\partial \alpha} \qquad C_{m_q} = \frac{\partial C_m}{\partial\left(\frac{\bar{c}\dot{\theta}}{2V}\right)}$$

$$C_{L_{\delta_e}} = \frac{\partial C_L}{\partial \delta_e} \qquad C_{m_{D_\alpha}} = \frac{\partial C_m}{\partial\left(\frac{\bar{c}\dot{\alpha}}{2V}\right)}$$

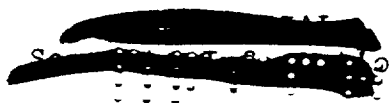

APPENDIX

METHOD OF COMPUTING TAKE-OFF PERFORMANCE

Equations of motion. The system of moving axes with the origin taken at the airplane center of gravity and the definition of forces and angles are shown in Figure 7. A summation of the inertia and external forces and moments acting at the center of gravity when the airplane is in the position indicated by the figure produces for the rigid landing-gear case

$$m\dot{V} = T\cos\alpha - D - W\sin\gamma + F_m\left[\sin(\gamma - \phi) - \mu\cos(\gamma - \phi)\right] \tag{1a}$$

$$mV\dot{\gamma} = L + T\sin\alpha - W\cos\gamma + F_m\left[\cos(\gamma - \phi) + \mu\sin(\gamma - \phi)\right] \tag{1b}$$

$$mk_Y^2\ddot{\theta} = M - F_m\left[(l_m + \mu h_m)\cos(\phi - \theta) + (h_m - \mu l_m)\sin(\phi - \theta)\right] \tag{1c}$$

The lift, drag, and pitching moment in terms of aerodynamic coefficients are

$$\left.\begin{aligned} L &= qSC_L \\ D &= qSC_D \\ M &= qS\bar{c}C_m \end{aligned}\right\} \tag{2}$$

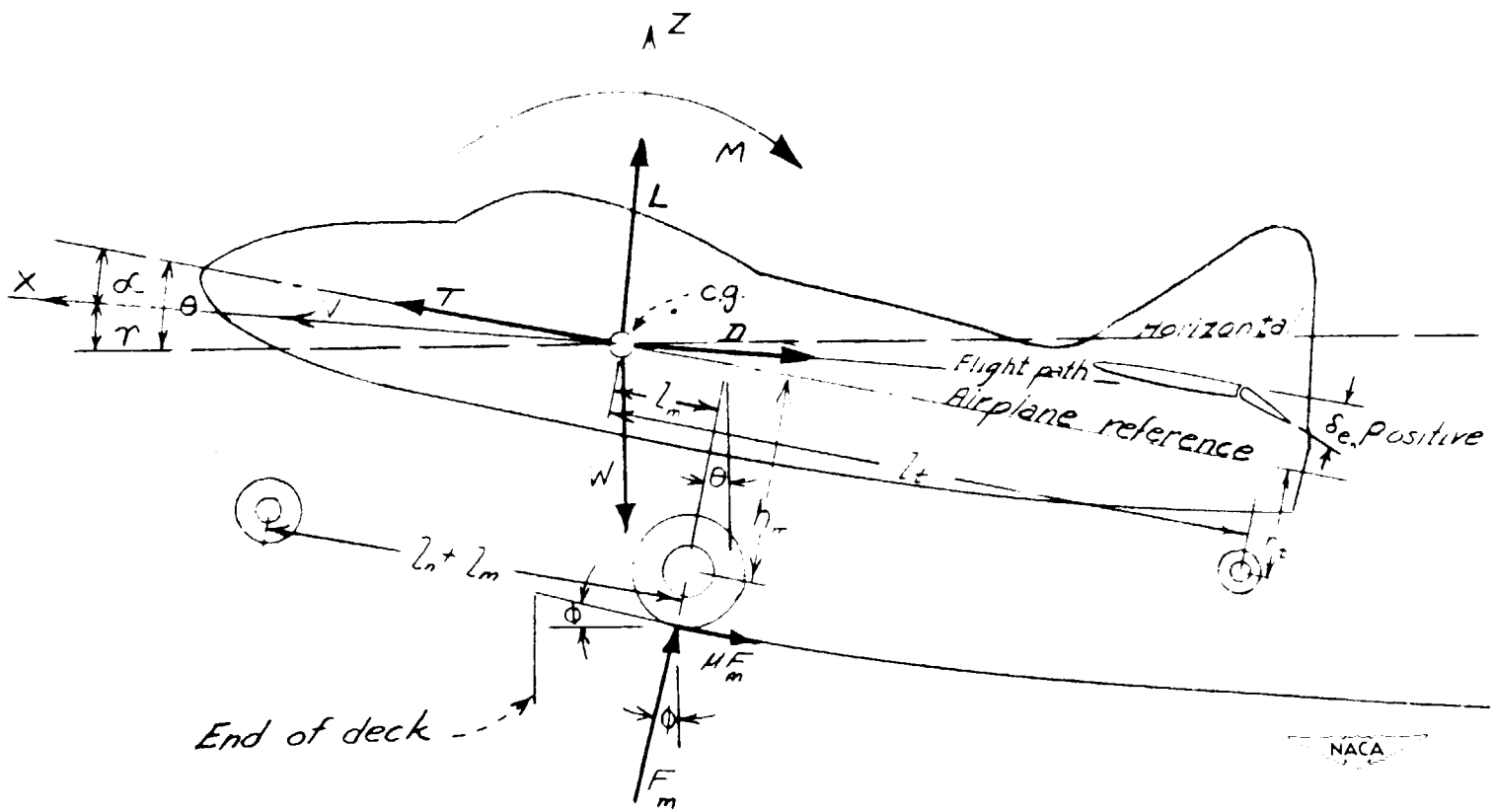

FIGURE 7

FORCES AND MOMENTS ACTING ON A CATAPULT-LAUNCHED AIRPLANE WHEN THE MAIN WHEELS ARE IN CONTACT WITH THE DECK

where

$$C_L = C_{L_o} + C_{L_{\delta_e}} \delta_e + C_{L_\alpha} \alpha$$

$$C_D = C_{D_o} + \frac{C_L^2}{\pi A e}$$

$$C_m = C_{m_o} + C_{m_{\delta_e}} \delta_e + C_{m_\alpha} \alpha + C_{m_q} \frac{\bar{c}}{2V} \dot{\theta} + C_{m_{D\alpha}} \frac{\bar{c}}{2V} \dot{\alpha}$$

The terms C_{L_o}, C_{D_o}, and C_{m_o} are the values of the coefficients when the variables upon which they depend are zero. The thrust of turbojet propelled airplanes is considered constant for the range of speeds involved.

If a tail wheel alone is in contact with the deck, the subscript m in equations (1) is replaced by t and the equations then define the motion after the main wheels leave the end of the deck. When all wheels are clear of the deck, the deck reaction force vanishes and the resulting equations of motion represent the airborne condition.

To simplify the analysis, the following general assumptions have been made:

(1) The controls are fixed.

(2) Unsteady lift effects are neglected.

(3) Angular displacements are small.

(4) A linear variation of lift and pitching moment with angle of attack is assumed.

(5) Rolling friction is neglected.

(6) Landing gear is assumed to be rigid.

Although the validity of some of these assumptions may be questioned, they are believed to be justified in this initial investigation which is primarily an evaluation of trends.

Airplane motion prior to take-off. To obtain particular solutions of the equations of motion representative of the airborne condition, it is necessary to determine the airspeed, angle of attack, attitude angle, and pitching velocity at the instant the wheels are clear of the deck. In computing these quantities, it was assumed that, during the take-off run, a distance of 50 feet, changes in angle of attack and attitude angle have a negligible effect upon acceleration due to thrust, and the variations of speed in this region do not affect pitching. Accordingly, the increment in airspeed was determined from equation (1a) and the angle of attack, attitude angle, and pitching velocity at the end of the deck were found by solving equations (1b) and (1c) simultaneously.

It was found convenient to express airspeed in terms of dynamic pressure and to use distance along the flight path as the independent variable rather than time. For the case of the straight deck, the terms γ and ϕ are zero

during the take-off run; therefore, when rolling friction is neglected, equation (1a) becomes

$$m\dot{V} = \frac{W}{g\rho}\frac{dq}{ds} = T - D$$

Assume the drag force to be constant during the take-off run. If, by definition, $s = (V_c + U)t$ and $x = V_c t$, the increment in q at the end of the straight deck ($x = 50$ feet) becomes

$$\Delta q = 50\ \rho g\left(\frac{V_c + U}{V_c}\right)\left(\frac{T - D}{W}\right) \tag{3}$$

For a corresponding take-off from the curved ramp, the increment in q is somewhat less because of the 1.73 feet of height gained. Equating the work required to lift the airplane 1.73 feet to the change in kinetic energy gives

$$\Delta q_{ramp} = -1.73\ \rho g$$

therefore at $x = 50$

$$q_{ramp} = q_{st.\ deck} - 1.73\ \rho g \tag{4}$$

Rewriting equations (1b) and (1c) in accordance with the assumptions of no rolling friction and small angles produces

$$\frac{W}{g}V\dot{\gamma} = L + T\alpha - W + F_m \tag{5a}$$

$$\frac{W}{g} k_Y^2 \ddot{\theta} = M - F_m l'_m \tag{5b}$$

where

$$l'_m = l_m + h_m(\phi - \theta)$$

The difference in the local deck angle and the airplane attitude angle, $(\phi - \theta)$, is practically constant during the take-off; therefore, l'_m may be satisfactorily approximated by its value at $x = 0$

$$l'_m = l_m - h_m\theta_1$$

It will be noted that equations (5) apply for the case in which the nose wheel is not touching the deck. Since the landing gear is assumed to be rigid, this condition exists whenever the aerodynamic pitching moment during take-off is sufficient to produce a nose-up pitching acceleration or when the nose wheel rolls from the end of the deck. In the case with the nose wheel in contact with the deck, the motion of the airplane before the nose wheel reaches the end of the deck is defined purely by the geometry of the take-off platform.

The normal acceleration at the center of gravity in g units may be expressed in terms of the radial acceleration of the ramp by the relation

$$\frac{V}{g} \dot{\gamma} = a_r + \frac{l'_m}{g} \ddot{\theta} \tag{6}$$

where

$$a_r = \frac{V_c^2}{gR}$$

When F in equations (5) is eliminated and the resulting equation is combined with equation (6), the pitching acceleration becomes

$$\ddot{\theta} = \frac{g}{l'_m{}^2 + k_Y{}^2}\left[\left(\frac{L + T\alpha}{W} - a_r - 1\right)l'_m + \frac{M}{W}\right] \qquad (7)$$

The angle-of-attack change during the take-off run is small and as a consequence changes in the lift and pitching moment in this region are neglected. The pitching acceleration given by equation (7) was therefore assumed to be constant over the region in which the nose wheel was free of the deck.

The values of α, θ, and $\frac{d\theta}{ds}$ at the instant the main wheels leave the deck ($x = 50$) may be computed from the following relations:

$$\left.\begin{aligned} \theta &= \theta_o + \dot{\theta}_o\,\Delta t + \frac{1}{2}\ddot{\theta}_o\,\Delta t^2 \\ \frac{d\theta}{ds} &= \frac{1}{V_c + U}\dot{\theta} = \frac{1}{V_c + U}\left[\dot{\theta}_o + \ddot{\theta}_o\,\Delta t\right] \\ \alpha &= \theta - \gamma \end{aligned}\right\} \qquad (8)$$

where γ is given by the ratio of vertical to horizontal components of air velocity at the center of gravity

$$\gamma = \frac{V_c\left(\frac{50}{R}\right) + l'_m\dot{\theta}}{V_c + U}$$

The term θ_o and its derivatives are evaluated at x_o, the distance between the bridle release point and the main wheels at the time the nose wheel leaves the deck. When these quantities are expressed in terms of the deck geometry, they may be written

$$\theta_o = \theta_i + \frac{x_o + \frac{l_m + l_n}{2}}{R}$$

$$\dot{\theta}_o = \frac{V_c}{R}$$

$$\ddot{\theta}_o = f(\alpha_o, \delta_e, R, V_c, U)$$

where in the latter equation

$$\alpha_o = \theta_o - \frac{V_o(x_o + l'_m)}{R(V_c + U)}$$

Aerodynamic damping in pitch is neglected in computing the motion prior to take-off.

When the pitching acceleration $\ddot{\theta}$ evaluated at the bridle release point is positive (nose up), the nose wheel lifts at $x = 0$ and Δt in equations (8) is given the value $\frac{50}{V_c}$. When the pitching acceleration is equal to or less than zero at the bridle release point, the nose wheel remains in contact with the deck until $x = 50 - (l_n + l_m)$ in which case $\Delta t = \frac{l_n + l_m}{V_c}$.

The quantities q, θ, α, and $\frac{d\theta}{ds}$ evaluated at the end of the deck by the preceding approximate relations (equations (3), (4), and (8)) were found to be in good agreement with an analytical solution of a linearized form of equations (1) in which the variations of lift, drag, and pitching moment during the take-off run were accounted for.

Airplane motion after take-off. In absence of deck reaction forces, equations (1) define airplane motion for the airborne condition. When it is noted that $\gamma = \theta - \alpha$, equations (1) and (2) combine to yield three simultaneous differential equations where the unknown variables are q, α, and θ. These equations are given below:

$$\left.\begin{aligned} \frac{dq}{ds} &= a_1 + q\left(a_2 + a_3\alpha + a_4\alpha^2\right) + a_5(\theta - \alpha) \\ \frac{d\alpha}{ds} &= a_6 + \frac{d\theta}{ds} + a_7\alpha + \frac{1}{q}\left(a_8 + a_9\alpha\right) \\ \frac{d^2\theta}{ds^2} &= a_{10} + a_{11}\alpha + a_{12}\frac{d\theta}{ds} + a_{13}\frac{d\alpha}{ds} + \frac{a_{14}}{q}\frac{dq}{ds}\frac{d\theta}{ds} \end{aligned}\right\} \quad (9)$$

in which

$$a_1 = \frac{\rho T}{m}$$

$$a_2 = -\frac{\rho S}{m}\left[C_{D_o} + \frac{\left(C_{L_o} + C_{L_{\delta_e}}\delta_e\right)^2}{\pi Ae}\right]$$

$$a_3 = \frac{\rho S}{m} \frac{2C_{L_\alpha}\left(C_{L_o} + C_{L_{\delta_e}}\delta_e\right)}{\pi Ae}$$

$$a_4 = -\frac{\rho S}{m} \frac{C_{L_\alpha}{}^2}{\pi Ae}$$

$$a_5 = -\frac{\rho W}{m}$$

$$a_6 = -\frac{\rho S\left(C_{L_o} + C_{L_{\delta_e}}\delta_e\right)}{2m}$$

$$a_7 = -\frac{\rho S C_{L_\alpha}}{2m}$$

$$a_8 = \frac{\rho W}{2m}$$

$$a_9 = -\frac{\rho T}{2m}$$

$$a_{10} = \frac{\left(C_{m_o} + C_{m_{\delta_e}}\delta_e\right)\rho S\bar{c}}{2mk_Y{}^2}$$

$$a_{11} = \frac{C_{m_\alpha} S\bar{c}\rho}{2mk_Y{}^2}$$

$$a_{12} = \frac{C_{m_q}\rho S\bar{c}^2}{4mk_Y{}^2}$$

$$a_{13} = \frac{C_{m_{D_\alpha}}\rho S\bar{c}^2}{4mk_Y{}^2}$$

$$a_{14} = \frac{1}{2}$$

Equations (9), subject to the initial conditions q, α, θ, and $\frac{d\theta}{ds}$ evaluated at the point where the airplane leaves the deck, were integrated on the Bell Telephone Laboratories X-66744 relay computer at the Langley Laboratory by using the Runge-Kutta[2] method of numerical integration.

[2] Scarborough, James B., Numerical Mathematical Analysis. The Johns Hopkins Press (Baltimore), 1930, pp. 299-303.